Recycled-Disposable-Chopstick-Fiber-Reinforced Polypropylene Green Composites

Yeng-Fong Shih,[1] Po-Wei Chen,[1] Chin-San Wu,[2] Chien-Ming Huang,[3] Chi-Fa Hsieh[4]

[1]*Department of Applied Chemistry, Chaoyang University of Technology, Wufong Township, Taichung County 41349, Taiwan*
[2]*Department of Chemical and Biochemical Engineering, Kao Yuan University, Kaohsiung County 82101, Taiwan*
[3]*Department of Chemical Engineering, Hsuiping Institute of Technology, Dali City, Taichung County 41280, Taiwan*
[4]*Chung Shan Institute of Science and Technology, Taoyuan County, Taiwan*

Received 7 February 2011; accepted 5 May 2011
DOI 10.1002/app.34857
Published online 2 September 2011 in Wiley Online Library (wileyonlinelibrary.com).

ABSTRACT: The utilization of disposable chopsticks is very popular in Taiwan, China, and Japan and is one of the major sources of waste in these countries. In this study, recycled disposable chopstick fiber was chemically modified. Subsequently, this modified fiber and polypropylene-*graft*-maleic anhydride were added to polypropylene (PP) to form novel fiber-reinforced green composites. A heat-deflection temperature (HDT) test showed an increase of approximately 81% for PP with the addition of 60-phr fibers, and the HDT of the composite could reach up to 144.8°C. In addition, the tensile strength, Young's modulus, and impact strength were 66, 160.3, and 97.1%, respectively, when the composite material was 40-phr fibers. Furthermore, this type of reinforced PP would be more environmentally friendly than an artificial-additive-reinforced one. It could also effectively reduce and reuse the waste of disposable chopsticks and lower the costs of the materials. © 2011 Wiley Periodicals, Inc. J Appl Polym Sci 123: 3046–3053, 2012

Key words: composites; fiber; recycling

INTRODUCTION

Disposable chopsticks are generally made from bamboo. The utilization of disposable chopsticks is very popular in Taiwan, China, and Japan and is one of the major sources of waste in these countries. Disposable chopsticks are common, everyday implements and are used in restaurants and for eating takeaway lunches bought at convenience stores and supermarkets. According to research by the Taiwan Environmental Protection Administration, the annual consumption of disposable chopsticks from 1999 to 2005 came to around 6.2 billion pairs (ca. 50,000 tons) in Taiwan. Even though the government has forbidden the use of disposable chopsticks in government organizations and school restaurants since 2006, the annual consumption of disposable chopsticks was still around 4.8 billion pairs (ca. 38,000 tons) in 2007. This amount of disposable chopsticks means that about 3 million bamboo plants were cut down. For this reason, determining how to recycle and reuse these disposable chopsticks has become an urgent research topic in chopstick-using countries and areas.[1–3]

As industry attempts to lessen the dependence on petroleum-based fuels and products, there is an increasing need to investigate more environmentally friendly, sustainable materials to replace existing materials. Recently, the utilization of plant fiber to reinforce the polymer matrix has been highly investigated for replacing synthetic fibers because of environmental demand. Composites of polypropylene (PP) and various natural fibers, such as pineapple leaf fibers, kenaf fibers, wood flour, rice hulls, newsprint fibers, hemp fibers, cotton fibers, and sunflower hull sanding dust, have been prepared by Arib and others.[4–10] Their results reveal that maleic anhydride grafted polypropylene (MAPP) is an effective compatibilizer for PP/natural fiber composites. Consequently, some improved mechanical properties were achieved.

In our previous studies, we also found that the mechanical and thermal properties of poly(butylene succinate),[11] poly(lactic acid),[12,13] and epoxy[14] were all promoted by the addition of water bamboo husk or recycled disposable chopstick fiber (RDCF). In this study, RDCF was incorporated into PP to enhance the mechanical and thermal properties of the plastics. Furthermore, the production of such green composites will lessen dependence on synthetic fibers and reduce the waste of disposable chopsticks.

Correspondence to: Y.-F. Shih (syf@cyut.edu.tw).
Contract grant sponsor: National Science Council of Taiwan; contract grant number: NSC 97-2221-E-324-001.

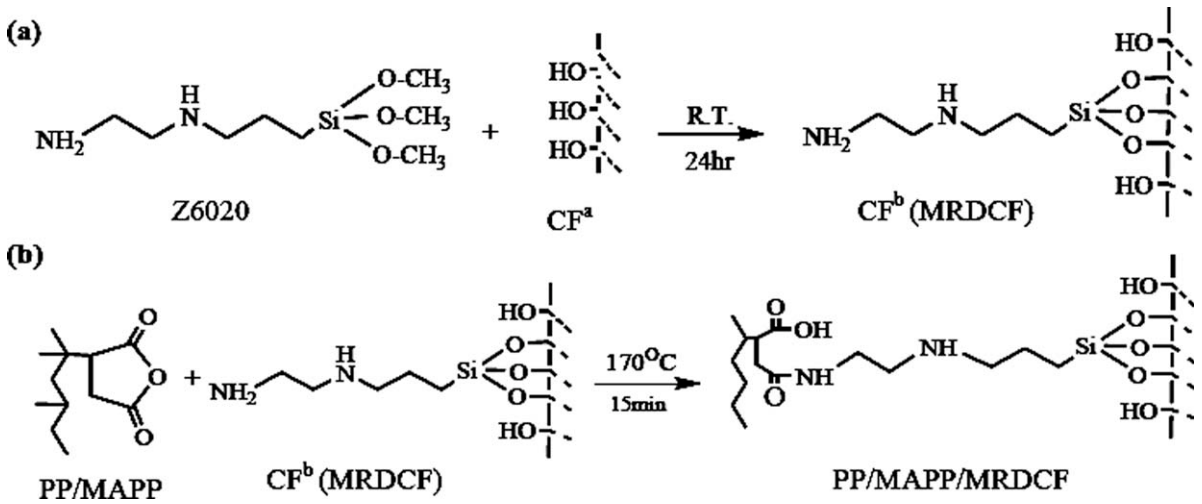

Scheme 1 Reactions of (a) coupling agent and CF[a] and (b) PP/MAPP and MRDCF (RT = room temperature).

EXPERIMENTAL

Materials

PP (PC366-5) was supplied by Taiwan LCY Chemical Industry Corp., Waltham, Massachusetts, USA, with a density of 0.903 g/cm^3 and a melt index (230°C/2.16 kg) of 5.5 g/10 min. MAPP (426512) was supplied by Sigma-Aldrich, Inc., with a density of 0.95 g/cm^3, a melt index (190°C/2.16 kg) of 115 g/10 min, and a content of maleic anhydride of about 0.6 wt %. To accelerate the separation of fiber and lignin, recycled disposable chopsticks (RDCs) were first forced between two rollers, of which one was fixed and the other was rotating. Subsequently, these RDCs were subjected to various surface chemical modifications, such as washing and alkali and coupling agent treatments. The procedures for the surface chemical modifications were as follows: The RDCs were washed with 2% detergent solution at 60°C for 1 h, then washed with distilled water, and finally dried in a vacuum oven at 80°C. The washed fibers were treated with a 25% NaOH solution for 2 h at 50°C, washed in running tap water, and then washed with distilled water until the pH value reached 7.0; this was followed by oven drying to obtain alkali-treated chopstick fibers (CF[a]'s). These fibers were then chopped by a pulverizer and screened by a 50-mesh sieve to obtain an average fiber diameter of 20 μm and a length of 1 cm and were subsequently treated by a silane coupling agent. The coupling agent [Z-6020, N—β-(aminoethy)-γ-aminopropyltrimethoxysilane] was supplied by Dow Corning Co. Surface treatment of the dried fiber was carried out in an acetone solution of silane. Fiber (5 g) and silane (0.5 g) were put in a flask with the proper volume of acetone. After agitation for 0.5 h, the flask was sealed with a polytetrafluoroethylene film and then kept for 12 h at room temperature. Then, the samples were washed with acetone to remove compounds not covalently bonded to the fiber and subsequently dried at 80°C in an oven to a constant weight. In this process, the coupling agent bonded to the surface of the fiber [Scheme 1(a)], and the chemically modified recycled disposable fiber (MRDCF) was obtained.

Preparation of the composites

PP, MAPP, and MRDCF were dried in an oven at 80°C for 48 h under reduced pressure until the moisture content was below 1.0 wt %. Immediately after drying, the PP was melt-blended with MAPP and fiber in a counterrotating internal mixer (Brabender PL2000, Duisburg, Germany) with a rotation speed of 60 rpm for 15 min at 200°C. In this step, the reaction of fiber grafting onto MAPP proceeded simultaneously, as shown in Scheme 1(b). Next, granulates of the previous mixture were obtained with a pulverizer. An injection molder with a 90-ton capacity was used to make dumbbell-shaped coupons for the mechanical property measurements. The amounts of fiber were 20, 40, and 60 phr on the basis of the weight of PP, and the formulations of the samples are shown in Table I.

Instruments

We obtained the infrared spectra with a Fourier transform infrared (FTIR) spectrometer (PerkinElmer

TABLE I
Formulations of the Samples (wt)

Sample	PP/MAPP(wt %)	Fiber (phr)
PP	100/0	0
PP/20CF*	95/5	20
PP/20CF	95/5	20
PP/40CF	95/5	40
PP/60CF	95/5	60

CF:MRDCF CF*: untreated RDCF

Paragon 500, Waltham, Massachusetts, USA) with a resolution of 2 cm^{-1} by scanning 50 times from 300 to 4000 cm^{-1} at room temperature. All of the film samples were carried out with the conventional NaCl disk method. The thermal behavior was investigated with a TA Instruments TGA Q50 thermogravimetric analyzer. All of the experiments were carried out under a nitrogen atmosphere at a purge rate of 100 mL/min. Samples of approximately 5 mg were heated to 500°C at a heating rate of 10°C/min. The phase-transition behavior was analyzed by a differential scanning calorimeter (TA Instruments DSC Q20). Moreover, the morphology was observed with a Carl Zeiss polarizing microscope equipped with a Mettler-Toledo hot stage. The PP samples were melted at 200°C for 5 min and then cooled down to 120°C at 20°C/min for isothermal crystallization to occur. A mechanical testing machine (Hung TA HT9102) was used to measure the tensile properties, according to ASTM D 638 standards. The notched Izod impact strength was measured with a GT-7045-MDL impact machine according to ASTM D 256 (Taichung, Taiwan). A GT-HV 2000 analyzer was used to measure the heat-deflection temperature (HDT) of the composites with a load of 66 psi, as specified by ASTM D 648. All of the results were taken as the average value of five samples. A Hitachi scanning electron microscope (model S-3000N) was used to evaluate the morphologies of the fibers and fractured surfaces of pure PP and the composites. The samples were sputter-coated with gold particles up to a thickness of about 10 nm before the surface characterization.

RESULTS AND DISCUSSION

FTIR spectrum

As shown in Figure 1, a strong and broad absorption was found at 3400 cm^{-1} for CF^a. This implied the presence of —OH groups in the fiber. Furthermore, the peaks at 3350, 3280, and 1660 cm^{-1} were found for Z6020. These were the characteristic absorption peaks of $—NH_2$ and —NH groups resulting from the silane coupling agent, Z6020. Moreover, the peaks at 1080 and 800 cm^{-1} were also found for Z6020. These were the characteristic absorption peaks of Si—O—Si and Si—OEt groups resulting from the silane coupling agent, Z6020. After treatment by the coupling agents, the absorption peak of —OH group in the fiber [alkali-silane-treated recycled disposable chopstick fiber (MRDCF or CF^b)] was shifted to a higher wave number near 3444 cm^{-1}. This implied that the degree of hydrogen bonding between —OH groups decreased after the coupling agent treatment and that the absorption peak of —OH groups was shifted to the position of free —OH groups (higher wave number).[15,16] Moreover, peaks at 1640, 1122, and 780 cm^{-1} were found for the treated fiber. These could have been due to the presence of —NH group and the asymmetric stretching of —Si—O—Si— and/or to the —Si—O—C— bonds.[17,18] They were indicative of the existence of polysiloxanes deposited on the fiber and confirmed the occurrence of a condensation reaction between the silane coupling agent and the fiber.

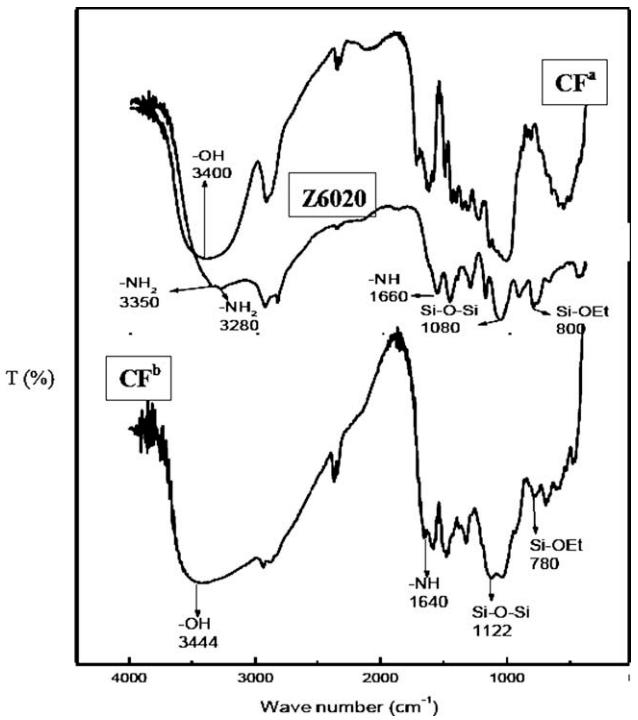

Figure 1 FTIR analysis of CF^a, Z6020, and MRDCF (CF^b).

The characteristic absorption peak of —C=O at 1710 cm^{-1} for MAPP is shown in Figure 2. Furthermore, the absorption peaks at 3436 cm^{-1} (—OH), 1706 cm^{-1} (—C=O), 1616 cm^{-1} (—NH), 1114 cm^{-1} (Si—O—Si), and 794 cm^{-1} (Si—OEt) for the PP/MAPP/MRDCF composite were related to the fiber, MAPP, and Z6020, respectively. It is important to note that the absorption peak of —OH groups in the composite shifted to a smaller wave number near 3436 cm^{-1}. Moreover, the absorption peak of —NH groups at 1640 cm^{-1} for MRDCF also shifted to 1616 cm^{-1}. This implied the formation of new hydrogen bonding between MRDCF and the polymer matrix; this would have further improved the compatibility of the composites.

Thermal analysis

Figure 3 and Table II reveal that the char yields (880°C) of the untreated recycled disposable chopstick fiber (CF*), CF^a, and CF^b were 7.0, 25.6, and 34.2%, respectively. Obviously, the char yields of the chemically treated fibers were larger than that of

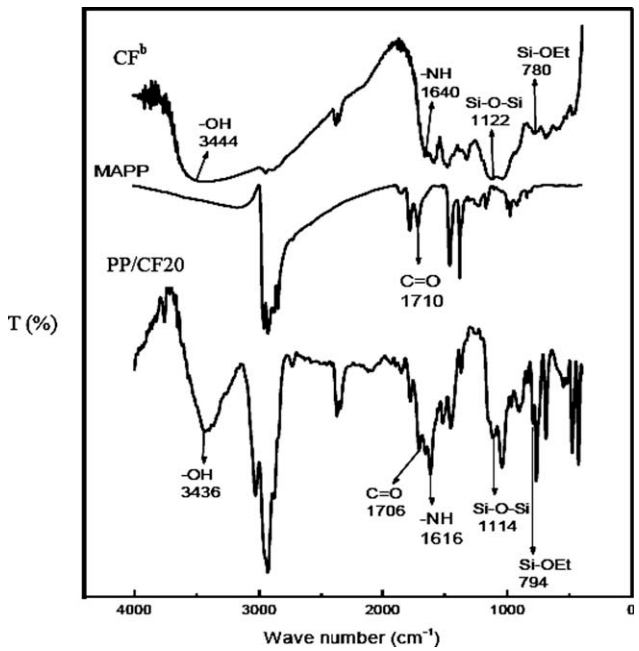

Figure 2 FTIR analysis of MRDCF (CF^b), MAPP, and PP/CF20 composite.

those left untreated. Moreover, the decomposition temperatures of the untreated fibers at different weight losses [5% (T_{d5}), 15% (T_{d15}), and 25% (T_{d25})] were all smaller than those that were chemically treated. The larger char yield and decomposition temperature of the chemically treated fibers revealed that the thermal stability of fiber was improved after the treatment process, especially by both alkali and silane treatment. Thermogravimetric analysis (TGA) thermograms of PP and the composites under nitrogen are shown in Figure 4. The decomposition temperatures (T_{d5} and T_{d25}) of MRDCF-reinforced composites were all smaller than those of pristine PP because of the nature of the plant. Plant fibers

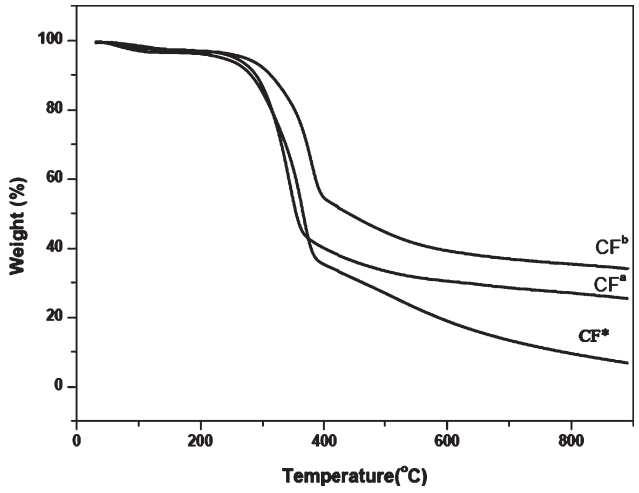

Figure 3 TGA thermograms of fibers by different surface treatments.

TABLE II
TGA Results of the Fibers with Different Surface Treatments

	T_{d5} (°C)	T_{d15} (°C)	T_{d25} (°C)	Char yield at 880°C (%)
CF*	233.3	299.9	320.3	7.0
CF^a	254.8	304.4	323.4	25.6
CF^b	270.5	334.9	363.3	34.2

would release absorbed moisture at about 40–140°C and proceed with the degradation process of cellulosic substances, such as hemicelluloses and cellulose, at about 140–370°C.[19] However, the char yields of the MRDCF-reinforced composites (Table III) were all larger than those of pristine PP. These results reveal that the addition of MRDCF to PP effectively raised the char yields of the samples. As reported previously,[20–22] the char yield is directly correlated to the potency of flame retardation for polymers. Increasing char formation can limit the production of combustible gases, decrease the exothermicity of the pyrolysis reaction, and inhibit the thermal conductivity of the burning materials.[23]

Figure 5 shows the differential scanning calorimetry thermograms for samples recorded during a cooling scan at a rate of 10°C/min. It was found that the crystallization temperature (T_c) increased with the addition of the fiber. This indicated that the fiber may have played a role as nucleating agent, enhanced the nuclei generation of the semicrystalline polymers in the crystallization process, and led to a higher crystallization rate at a higher temperature.[24]

Mechanical properties

Table IV shows that the mechanical strengths of RDCF-reinforced PP composites were all larger than that of pristine PP. The performance of the MRDCF-containing composite (PP/CF20) was better than

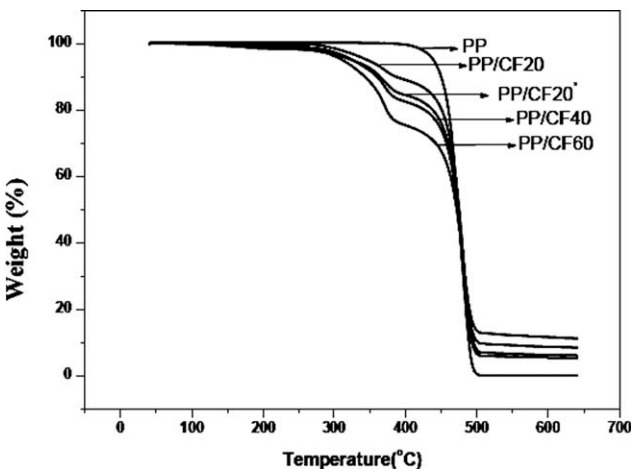

Figure 4 TGA thermograms of PP and the composites.

TABLE III
TGA Results of PP and the Composites

	T_{d5} (°C)	T_{d25} (°C)	Char yield at 600°C (%)
PP	439.9	463.6	0.2
PP/CF20*	326.2	452.8	5.5
PP/CF20	347.8	459.0	6.3
PP/CF40	327.3	448.4	8.8
PP/CF60	312.9	405.7	11.7

that of the untreated fiber containing one (PP/CF20*). This indicated that the chemical treatment of fiber effectively enhanced the adhesion between the fiber and polymer matrix, so the mechanical properties of the composites were significantly improved. For PP/CF40, the increments of tensile strength, Young's modulus, and impact strength were 66, 160.3, and 97.1%, respectively, compared to neat PP. However, the strengths of PP/CF60 were somewhat smaller than that of PP/CF40. This may have been due to the aggregation of fibers or poor adhesion between the fibers and the polymer matrix resulting from the high content of the fibers. This was confirmed by scanning electron microscopy (SEM) analysis.

Theoretical modeling of the tensile modulus of the PP-based composites

Halpin–Tsai and Tsai–Pagano equations[25,26] were used to determine the theoretical values of the Young's moduli of MRDCF-reinforced PP composites. Halpin–Tsai equations can predict the theoretical values of the longitudinal modulus (E_{11}) and transverse modulus (E_{22}) of short-fiber composites. The equations for E_{11} and E_{22} can be expressed as

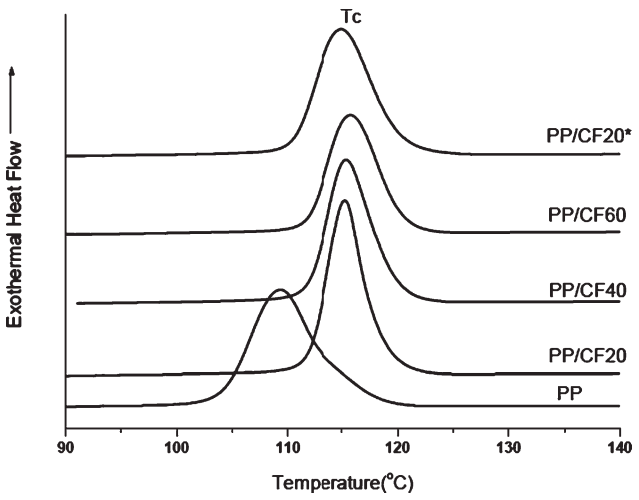

Figure 5 Differential scanning calorimetry thermograms of the samples (cooling rate = 20°C/min).

TABLE IV
Mechanical Properties of PP and the Composites

	Tensile strength (MPa)	Increment (tensile strength; %)	Impact (J/m)	Increment (impact strength; %)
PP	31.5 ± 0.8	-	24.5 ± 1.0	—
PP/CF20*	37.2 ± 1.5	17.9	25.2 ± 2.1	2.9
PP/CF20	39.7 ± 0.4	26.1	31.9 ± 1.6	31.2
PP/CF40	51.9 ± 0.6	66.0	48.3 ± 1.4	97.1
PP/CF60	49.0 ± 0.8	55.4	45.3 ± 1.3	84.9

$$E_{11} = E_m \frac{1 + \xi\eta V_f}{1 - \eta V_f} \tag{1}$$

$$E_{22} = E_m \frac{1 + 2\eta^* V_f}{1 - \eta^* V_f} \tag{2}$$

where

$$\eta = \frac{\left(\frac{E_f}{E_m}\right) - 1}{\left(\frac{E_f}{E_m}\right) + \xi} \tag{3}$$

$$\eta^* = \frac{\left(\frac{E_f}{E_m}\right) - 1}{\left(\frac{E_f}{E_m}\right) + 2} \tag{4}$$

where η is an efficiency factor for the longitudinal modulus (E_{11}), η^* is an efficiency factor for the transverse modulus (E_{22}), E_f (18.5 GPa), E_m (1.21 GPa), and V_f denote the Young's moduli of the fiber and the matrix and the volume fraction of the fiber, respectively. ξ is a measure of the geometry of reinforcement. If the fiber is rectangular in cross section, ξ may be calculated as

$$\xi = 2(l/d) \tag{5}$$

where l/d is the aspect ratio of the reinforcement. The in-plane modulus of a random fiber composite (E_{random}) was proposed by Tsai and Pagano[27] to be

$$E_{\text{random}} = \frac{3}{8}E_{11} + \frac{5}{8}E_{22} \tag{6}$$

The densities of PP and MRDCF were 0.93 and 1.21 g/cm^3, respectively, and the average aspect ratio of MRDCF was about 40. A comparison between the theoretical and experimental Young's moduli of the PP composites as a function of the fiber volume fraction is given in Figure 6. The results reveal good fitting for the MRDCF/PP composites at a fiber volume fraction lower than 0.25. However, there was considerable deviation in experimental values compared to the theoretical values of Young's modulus for the MRDCF/PP composites at a fiber volume

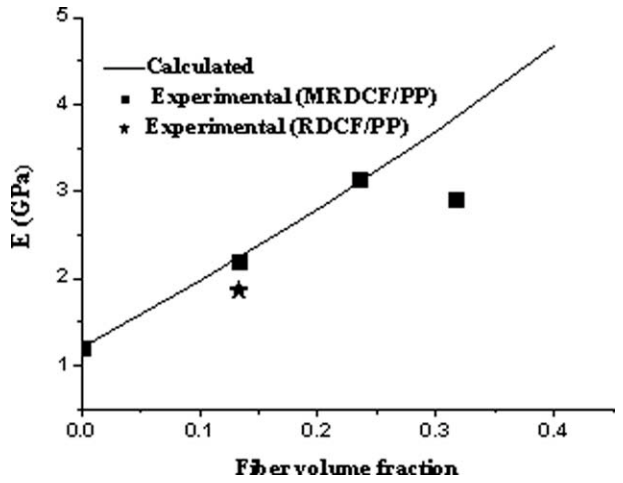

Figure 6 Comparison of the theoretical and experimental Young's moduli of the PP composites as a function of the fiber volume fraction.

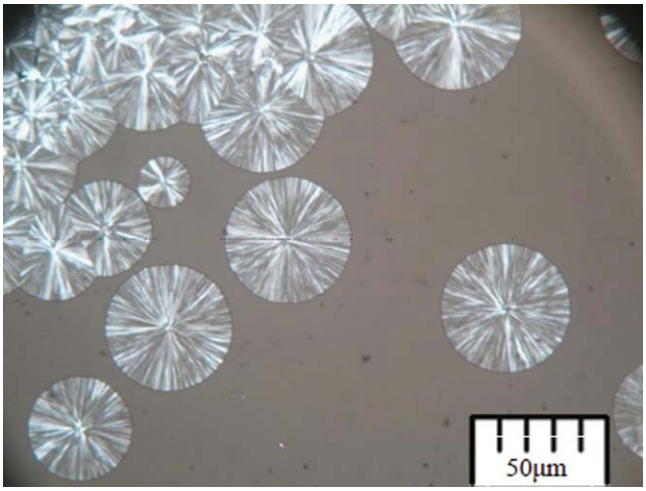

Figure 7 POM micrograph of pristine PP. [Color figure can be viewed in the online issue, which is available at wileyonlinelibrary.com.]

fraction larger than 0.3 and the RDCF-reinforced PP composites because of the aggregation of fibers or low compatibility between the untreated fiber and matrix. This could have reduced their reinforcing effect in the PP-based composites.

HDT

HDT is defined as the temperature at which a material deflects by 0.25 mm under the application of a load (66 psi). Table V gives the values of the HDTs of the RDCF-reinforced PP composites. HDT showed a significant increase of about 27–65°C with the addition of fibers, and the values increased with increasing fiber content. Particularly, for PP/CF60, the increment of HDT was 81% compared to neat PP and reached up to 144.8°C. The HDT value depends on the modulus and glass-transition temperature of a material. The modulus–temperature relationship plays a critical role in determining the HDT. We correlated the improvement in the HDT values for the PP-based composites to the higher modulus values of these composites at elevated temperatures compared to pristine PP (Table IV).[28] Because HDT is a key property in selecting materials for commercial and industrial applications, the improvement of a composite's HDT could open up new uses for PP.

TABLE V
HDTs of PP and the Composites

	HDT(°C)	Increment (HDT; %)
PP	80	—
PP/CF20*	106.9	33.6
PP/CF20	122.2	52.8
PP/CF40	138.5	73.1
PP/CF60	144.8	81.0

For example, it can be used for hot-liquid filling, high-temperature packing bags, or high-temperature PP pump tubes for transferring high-temperature corrosive liquids.

Polarizing optical microscopy (POM) analysis

To understand the crystallization behavior, POM was used to compare the crystal morphology of PP and the PP/MRDCF composites. The optical micrographs of the crystalline growth at T_c (120°C) for the pristine PP sample and fiber-containing composite are shown in Figures 7 and 8. The spherulites were found in the matrices of pristine PP (Fig. 7). On the other hand, the smaller and less ordered crystals were found in the micrograph of the composite (Fig. 8). These results revealed that the RDCF acted as a

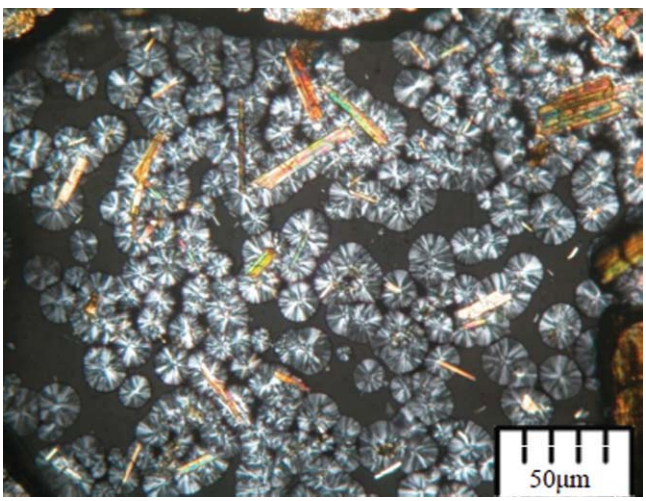

Figure 8 POM micrograph of PP/CF20. [Color figure can be viewed in the online issue, which is available at wileyonlinelibrary.com.]

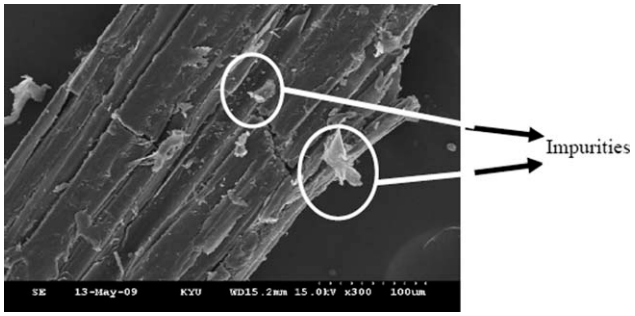

Figure 9 SEM micrograph of the untreated fiber.

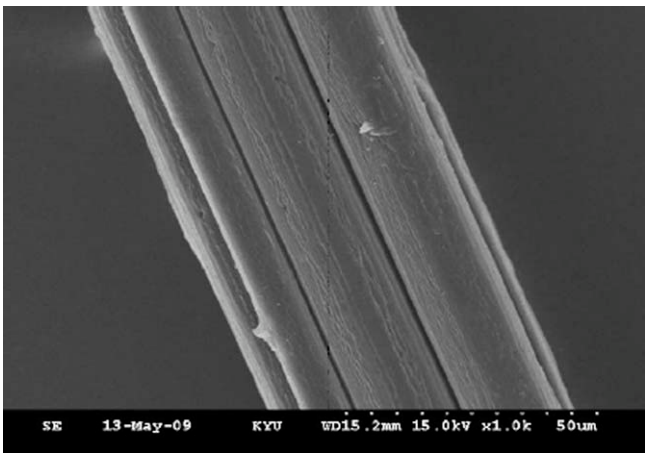

Figure 10 SEM micrograph of CF[a].

nucleating agent to increase the number of the nuclei and caused the formation of smaller spherulites. It is known that when heterogeneous nucleation occurs with a sufficiently high density along the polymer–fiber interface, the resulting crystal growth is restricted to the lateral direction so that a columnar layer develops around the fiber.[29]

SEM analysis

The SEM photographs of CF*, CF[a], and MRDCFs are shown in Figures 9–11. The surface of the untreated fiber was covered with some impurities and was not as smooth (Fig. 9), whereas CF[a] exhibited a cleaner and neater appearance (Fig. 10). Figure 11 reveals that the fiber seemed muffled by a thin layer after the silane treatment.

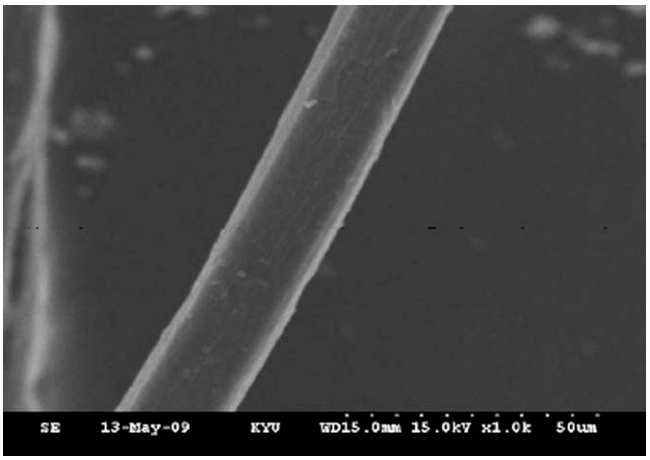

Figure 11 SEM micrograph of CF[b].

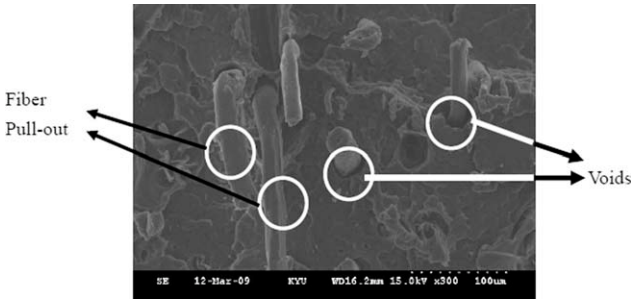

Figure 12 SEM micrograph of the fracture surface of the untreated RDCF containing sample (PP/CF20*).

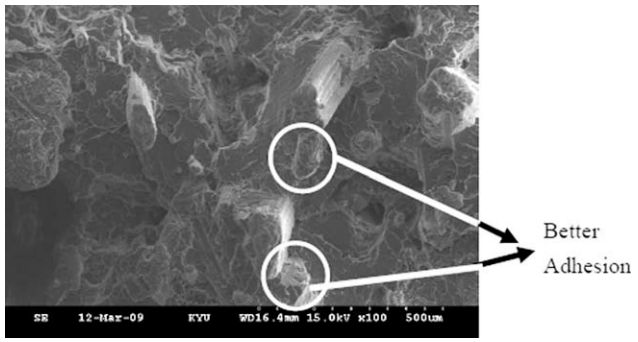

Figure 13 SEM micrograph of the fracture surface of the MRDCF-containing sample (PP/CF20).

The SEM photograph of the untreated fiber reinforced PP matrix is shown in Figure 12. The compatibility between the untreated fiber and PP matrix was poor, as evidenced by the presence of pull-out fiber and voids on the fracture surface. The compatibility between the fiber and PP matrix was improved when the fiber was treated by silane coupling agents, as shown in Figure 13. This was shown by the densely knitted texture. This implied that the

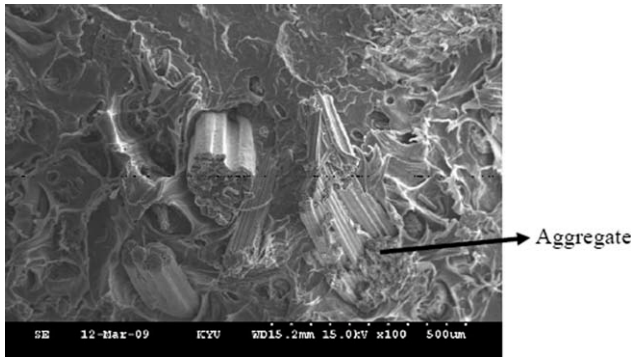

Figure 14 SEM micrograph of the fracture surface of the MRDCF-containing sample (PP/CF60).

coupling agents played an important role as compatibilizers between the fiber and the polymer matrix and led to better adhesion. However, aggregates were found when the content of silane-treated fiber was as large as 60 phr (Fig. 14). This corroborated the results of the mechanical analysis, which showed that the poor adhesion of the fiber to the matrix decreased the tensile and impact strengths of the composite.

CONCLUSIONS

The addition of MRDCFs to PP provided a vehicle for improving the mechanical and thermal properties. With the addition of the fibers, the char yields of the composites were increased. Moreover, the maximum increments of the tensile and impact strengths of PP were approximately 66 and 97.1%, respectively. Furthermore, HDT significantly increased by about 81% compared to neat PP and reached up to 144.8°C. These improvements could open up new uses for PP. This type of reinforced plastic not only exhibits excellent properties but also is more environmentally friendly than the artificial-additive-reinforced ones and can reduce and reuse the waste from disposable chopsticks.

References

1. Disposable Chopsticks 2003, Japanese Market News. http://www.ibpcosaka.or.jp/network/e_trade_japanesemarket/household_products/disposable_chopsticks03.html. Accessed on Oct 11, 2003.
2. Giving Disposable Chopsticks a Life Cycle, JFS Newsletter. http://www.japanfs.org/en/mailmagazine/newsletter/pages/027818.html. Accessed on Dec 2006.
3. Big in Japan: Making Biofuel Out of Used Chopsticks. http://www.gadling.com/2007/08/27/big-in-japan-making-biofuel-out-of-used-chopsticks. Accessed on Aug 27, 2007.
4. Arib, R. M. N.; Sapuan, S. M.; Ahmad, M. M. H. M.; Paridah, M. T.; Zaman, H. M. D. K. Mater Des 2006, 27, 391.
5. Tajvidi, M.; Falk, R. H.; Hermanson, J. C. J Appl Polym Sci 2006, 101, 4341.
6. Zampaloni, M.; Pourboghrat, F.; Yankovich, S. A.; Rodgers, B. N.; Moore, J.; Drzal, L. T.; Mohanty, A. K.; Misra, M. Compos A 2007, 38, 1569.
7. Pickering, K. L.; Beckermann, G. W.; Alam, S. N.; Foreman, N. J. Compos A 2007, 38, 461.
8. Beckermann, G. W.; Pickering, K. L. Compos A 2008, 39, 979.
9. Kim, S. J.; Moon, J. B.; Kim, G. H.; Ha, C. S. Polym Test 2008, 27, 801.
10. Sui, G.; Fuqua, M. A.; Ulven, C. A.; Zhong, W. H. Bioresour Technol 2009, 100, 1246.
11. Shih, Y. F.; Lee, W. C.; Jeng, R. J.; Huang, C. M. J Appl Polym Sci 2008, 99, 188.
12. Wang, K. H.; Wu, T. M.; Shih, Y. F.; Huang, C. M. Polym Eng Sci 2008, 48, 1833.
13. Shih, Y. F.; Huang, C. C.; Chen, P. W. Mater Sci Eng A 2010, 527, 1516.
14. Shih, Y. F. Mater Sci Eng A 2007, 445–446, 289.
15. Wu, H. D.; Chu, P. P.; Ma, C. C. M.; Chang, F. C. Macromolecules 1999, 32, 3097.
16. Shih, Y. F.; Jeng, R. J. Polym Int 2004, 53, 1892.
17. Britcher, L.; Kehoe, D.; Matisons, J.; Swincer, G. Macromolecules 1995, 28, 3110.
18. Pouchert, C. J. The Aldrich Library of Infrared Spectra, 3rd ed.; Aldrich Chemical: Milwaukee, WI, 1985; pp 62, 123, 1535.
19. Pan, P.; Zhu, B.; Kai, W.; Serizawa, S.; Iji, M.; Inoue, Y. J Appl Polym Sci 2007, 105, 1511.
20. Shih, Y. F.; Jeng, R. J. J Appl Polym Sci 2002, 86, 1904.
21. Wu, C. S.; Liu, Y. L.; Hsu, K. L. Polymer 2003, 44, 565.
22. Shih, Y. F.; Wang, Y. T.; Jeng, R. J.; Wei, K. M. Polym Degrad Stab 2004, 86, 339.
23. Pearce, E. M.; Leipins, R. Environ Health Persp 1975, 11, 59.
24. Kawamoto, N.; Sakai, A.; Horikoshi, T.; Urushihara, T.; Tobita, E. J Appl Polym Sci 2007, 103, 244.
25. Halpin, J. C. J Compos Mater 1969, 3, 732.
26. Halpin, J. C.; Kardos, J. L. Polym Eng Sci 1976, 16, 344.
27. Tsai, S. W.; Pagano, N. J. Invariant Properties of Composite Materials: Composite Materials Workshop; Technomic: Stamford, CT, 1968.
28. Nielsen, E. L. Mechanical Properties of Polymers and Composites; Marcel Dekker: New York, 1976, Vol. 2.
29. Hermida, E. B.; Mega, V. I. Compos A 2007, 38, 1387.